Design and analysis of a phase modulator based on a metal–polymer–silicon hybrid plasmonic waveguide

Xiaomeng Sun, Linjie Zhou,* Xinwan Li, Zehua Hong, and Jianping Chen

State Key Laboratory of Advanced Optical Communication Systems and Networks, Department of Electronic Engineering, Shanghai Jiao Tong University, Shanghai 200240, China

*Corresponding author: ljzhou@sjtu.edu.cn

Received 28 February 2011; revised 16 May 2011; accepted 18 May 2011; posted 20 May 2011 (Doc. ID 143309); published 1 July 2011

A plasmonic-hybrid-waveguide-based optical phase modulator is proposed and analyzed. The field enhancement in the low-index high-nonlinear polymer layer provides nanoscale optical confinement and a fast optical modulation speed. At 2.5 V drive voltage, a π phase shift can be obtained for a 13-μm-long plasmonic waveguide. Because of its small capacitance and parasitic resistance, the modulation bandwidth can reach up to 100 GHz with a low power consumption of ~9 fJ/bit. The plasmonic waveguide is connected to a silicon wire waveguide via an adiabatic taper with a coupling efficiency of ~91%. The phase modulator can find potential applications in optical telecommunication and interconnects. © 2011 Optical Society of America

OCIS codes: 240.6680, 250.2080, 250.5300, 230.2090.

1. Introduction

With the advances in optical signal processing and interchip/intrachip optical interconnections, waveguide-based photonic devices are of great importance for the development of highly compact nanophotonic integrated chips. However, due to the diffraction limit, conventional dielectric waveguides have mode sizes not smaller than half of the wavelength. In order to break the diffraction limit to improve the integration density, surface plasmon polaritons (SPPs) have recently been employed to implement various integrated plasmonic devices. SPPs, as the electromagnetic (EM) excitations coupled to surface collective oscillations of free electrons in a metal, are bound to and propagate along metal–dielectric interfaces. SPPs have extremely short wavelengths, high optical field enhancement at the interface, and strong optical confinement down to deep subwavelength dimensions [1–14]. There are various types of SPP-based plasmonic waveguides, including groove waveguides [4–6], slot waveguides [7–9], gold strip waveguides [10], and hybrid plasmonic waveguides [11–14]. However, so far, most of the plasmonic waveguides proposed and demonstrated have been passive ones with their propagation constants fixed, which greatly limits their functionalities.

On the other hand, silicon photonics is one of the most promising candidate technologies for optical telecommunication and interconnects. Optical modulators, including amplitude, phase, and polarization modulators, are the workhorses for such applications [15]. Si-based optical modulators have been demonstrated using the free-carrier plasma dispersion effect [16] and the thermo-optic effect [17]. The Kerr and Franz–Keldysh effects can also be employed, but these effects are relatively weak in pure silicon at telecommunication wavelengths [16]. The Pockels effect in $LiNbO_3$ and polymer materials is widely used to realize high-speed electro-optic modulators [18,19]. In particular, poled polymers exhibit a very high electro-optic coefficient r_{33}, enabling optical modulation with low drive voltage. However, in silicon, due to its centrosymmetric crystal structure, the Pockels effect is absent and cannot be used to realize optical modulation.

0003-6935/11/203428-07$15.00/0

Here we present an optical phase modulator based on a silicon–polymer hybrid plasmonic waveguide to fully utilize the high electro-optic effect of the polymer material to realize high-speed and low-power optical modulation. The plasmonic waveguide is composed of a metal–polymer–silicon (MPS) stack to form high optical confinement in the nanometer-sized polymer layer. The effective refractive index of the plasmonic waveguide can be changed by an external voltage applied on the MPS structure. The plasmonic waveguide is connected with a silicon wire waveguide through two adiabatic tapers, making it accessible by silicon wire waveguides.

2. Device Structure

Figure 1(a) shows the schematic perspective view of the proposed active plasmonic waveguide connected with a silicon wire waveguide. Figure 1(b) is the cross-sectional view of the plasmonic waveguide comprising silicon (Si), polymer, and silver (Ag) layers. For the transverse electric (TE) polarization, surface plasmon waves can be excited at the sidewall metal–polymer interfaces. To reduce the absorption loss from the top metal layer, a thick SiO_2 cap is placed on top of the waveguide. In our simulation, we choose silver as the metal material with permittivity $\varepsilon_{Ag} = -133.75 + 3.337i$ around the 1550 nm wavelength [20], and its thickness is W_{Ag}. The polymer layer is assumed to have a refractive index $n_{polymer} = 1.6$ and its thickness is $W_{polymer}$. The silicon waveguide core width and height are W_{si} and H_{si}. The refractive indices for SiO_2 and Si are $n_{SiO2} = 1.46$ and $n_{Si} = 3.48$.

We use the electro-optic effect in $\chi^{(2)}$ nonlinear polymer to actively tune the plasmonic mode. As the thin polymer layer is sandwiched between the silicon and silver layers, the plasmonic waveguide structure naturally forms a capacitor with the silicon and silver layers as the two capacitor plates. The silicon core is intentionally n-type doped with a doping concentration of $2 \times 10^{20}\ cm^{-3}$ to reduce its resistivity and improve the modulation speed. Once an external voltage is applied onto the capacitor, the refractive index of the poled polymer changes accordingly due to its strong $\chi^{(2)}$ nonlinear electro-optic effect. Because the silicon waveguide core is wrapped by the polymer and SiO_2 layers, we design finger-shaped access bridges [21] at the input and output ends to connect the silicon core out to an electrode as shown in Fig. 1(a).

3. Simulation Results

A. Hybrid Plasmonic Mode

For dielectric waveguides, light is strongly confined in the high-index dielectric layers due to total internal reflection. However, for the proposed hybrid plasmonic waveguide, the intensity maxima are located in the low-index sidewall polymer for TE polarization [14]. The field in the polymer nanoslots is greatly enhanced due to SPP excitation at the Ag–polymer interface and the electric field discontinuity at the Si–polymer interface.

We use the finite element method (FEM) to numerically calculate the hybrid plasmonic waveguide modes at the 1550 nm wavelength. The FEM is used to solve the partial differential equations by meshing a continuous domain into a set of discrete subdomains. The grid size is set to be 10 times smaller than the dimensions of the corresponding regions to get accurate simulation results within the allowed time and computational resources. The domain of the solution is meshed into triangular elements with quartic Lagrange functions. When W_{Si} is small ($\lesssim$200 nm), the plasmonic waveguide can support only one mode, with its major electric field evenly distributed in the two nanoslots (even mode). When the core width W_{Si} increases, the mode with its major electric field opposite in the two nanoslots (odd mode) appears. Figure 2 shows the major electric field $E_x(x,y)$ pattern for the plasmonic waveguide. The geometric parameters are chosen as $W_{Si} = 250$ nm, $W_{polymer} = 20$ nm, and $W_{Ag} = 10$ nm, and the top SiO_2 cap thickness as 100 nm. The even and odd modes both exist in this waveguide. The complex effective refractive index of the hybrid plasmonic waveguide mode can be expressed as $n_{eff} = n_{re} + in_{im}$, where the real part n_{re} is associated with the light propagation constant and the imaginary part n_{im} with the propagation loss. The propagation loss is given as $20\log(e)k_0 n_{im}$, where k_0 is the free-space wavenumber.

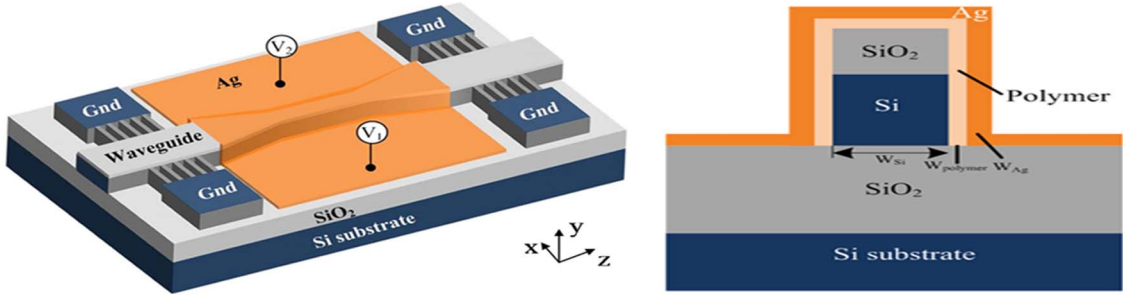

(a) (b)

Fig. 1. (Color online) (a) Schematic perspective view of the proposed phase modulator based on a hybrid plasmonic waveguide. (b) Cross-sectional view of the hybrid plasmonic waveguide.

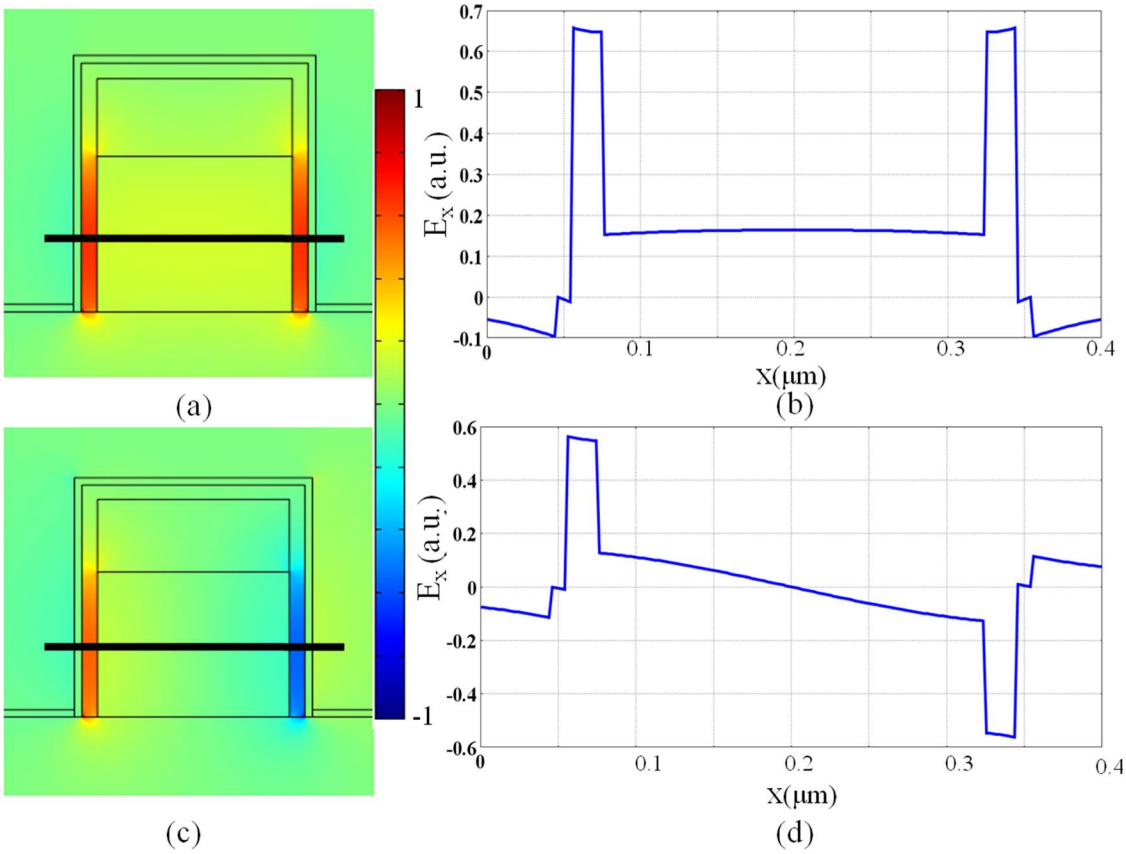

Fig. 2. (Color online) (a) and (c) Transverse electric field mode pattern for (a) even and (c) odd modes. (b) and (d) Electric field distribution along a horizontal line for the even and odd modes.

Figure 3(a) shows that n_{re} of the even mode changes with W_{Si}. Here, $W_{Ag} = 10$ nm and the polymer widths are chosen as $W_{polymer} = 10$, 20, and 50 nm. It can be seen that n_{re} increases with W_{Si} when the polymer layer is thick, while it decreases with W_{si} when the polymer layer is thin. For a given W_{Si}, n_{re} becomes larger for a thinner polymer layer. Note that, when the polymer layer is very thin and less than a critical value, the metal–polymer–silicon stack at each side can itself support a hybrid SPP mode with $n_{re} > n_{si}$ [22] (for a 5 nm polymer layer, n_{re} is 4.38). Our plasmonic waveguide thus can be regarded as a coupled hybrid SPP system with its mutual coupling enabled through the central silicon strip. The strong coupling results in a mode splitting into even and odd polarities. On the other hand, upon mode coupling, the otherwise leaky hybrid SPP mode existing for a large polymer width [22] becomes a guided one, because the radiation wave is now confined in the silicon core. There is no cutoff for the even mode in our hybrid plasmonic waveguide. Figure 3(b) shows the propagation loss of the even mode changes with the silicon core width W_{Si}. For a given W_{Si}, one has a large propagation loss for a small polymer width, because the optical field at the Ag–polymer interface is increased. Figures 3(c) and 3(d) show the effective refractive index and the propagation loss change with the silicon core width W_{Si} for the odd mode. In comparison, the even mode has a higher effective refractive index and lower propagation loss, so we choose the even mode to implement the phase modulation. In order to excite the even hybrid plasmonic mode, we use an adiabatic taper to gradually transform the photonic mode in the silicon waveguide to the hybrid plasmonic mode in the phase modulator (see Subsection 3.C).

B. Phase Modulation

As the polymer has a high electro-optic effect, the refractive index of the polymer has a relatively large change upon an external voltage, resulting in a significant effective index change and, hence, a large phase shift after a certain propagation length. Nonlinear polymers typically have a very high resistivity of 10^{11} Ω·cm [23], and as a result, the silicon and metal layers are electrically isolated and can be used as the modulator electrodes. We consider the molecular glasses based on the reversible self-assembly of aromatic/perfluoroaromatic dendron-substituted nonlinear optical chromophores as the electro-optic polymer, which has an electro-optic coefficient $r_{33} > 200$ pm/V with good alignment stability [24]. The polymer refractive index change Δn to an external electric field E is given by [18]

$$\Delta n = -r_{33} n^3_{\text{polymer}} E/2, \tag{1}$$

$$E = U/W_{\text{polymer}}, \tag{2}$$

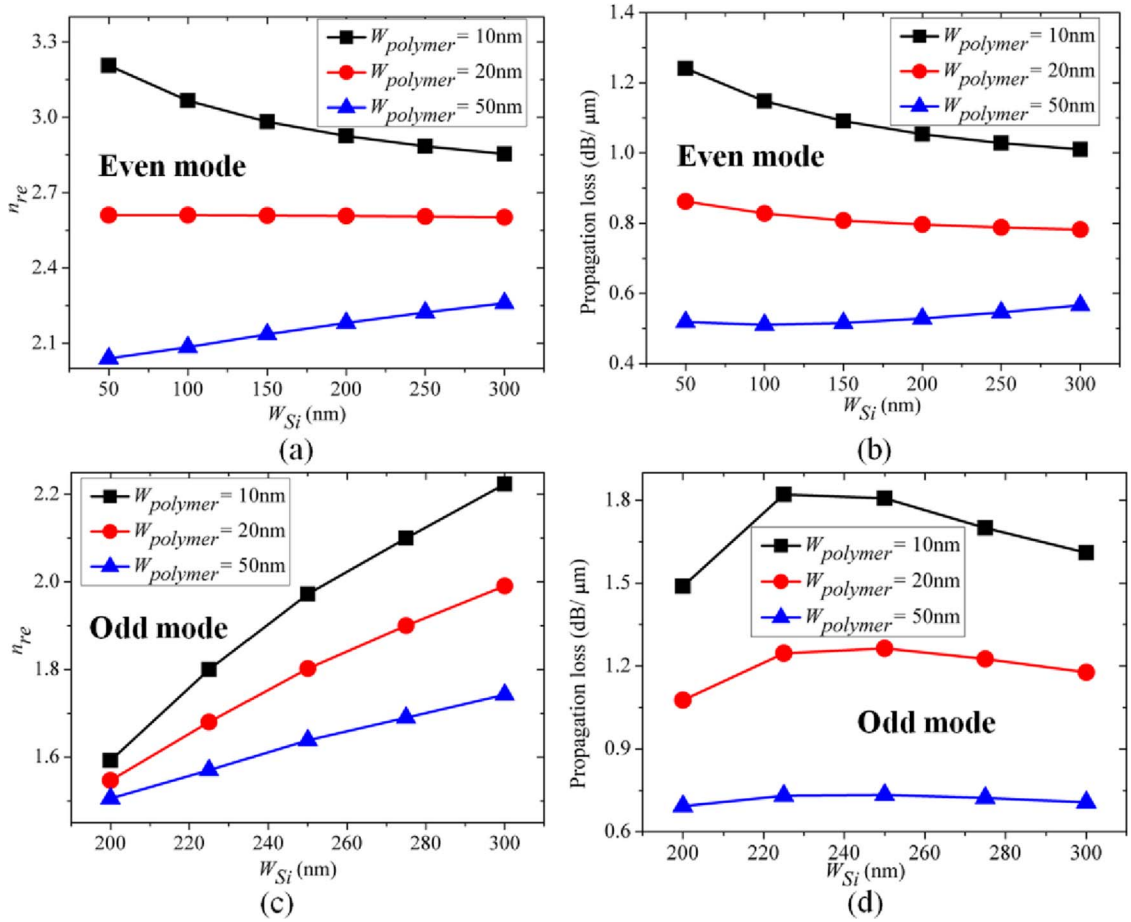

Fig. 3. (Color online) (a) and (c) n_{re} changes as a function of W_{Si} for the even and odd modes. (b) and (d) Propagation loss changes as a function of W_{Si} for the even and odd modes. Here $W_{\mathrm{Ag}} = 10\,\mathrm{nm}$, and the polymer widths are $W_{\mathrm{polymer}} = 10$, 20, and 50 nm.

where U is the voltage applied on the polymer layer. The change in the effective refractive index results in a phase shift $\Delta\Phi$ in the waveguide: $\Delta\Phi = 2\pi\Delta n_{\mathrm{re}} d/\lambda$, where d is the length of the hybrid plasmonic waveguide in the phase modulator, λ is the wavelength of light in free space, and Δn_{re} is the real part of the effective refractive index change in the waveguide. We consider only the even hybrid plasmonic mode (the fundamental mode) for the phase modulation. Considering the fabrication limit, we choose a set of geometric parameters that can be achieved using the existing technologies in analyzing the proposed structure. Figure 4(a) shows that Δn_{re} changes with the silicon core width W_{Si}. The silver layer width is $W_{\mathrm{Ag}} = 10\,\mathrm{nm}$ and the polymer widths are $W_{\mathrm{polymer}} = 10$, 20, and 50 nm. The applied voltage between the silicon and the metal electrodes is 0.5 V. The sidewall polymer width plays an important role in the phase modulator. Δn_{re} decreases with both W_{polymer} and W_{Si}. Therefore, in order to more efficiently change the effective refractive index of the hybrid plasmonic mode using the polymer linear electro-optic effect, thin polymer and silicon layers should be chosen. Figure 4(b) shows that the phase shift $\Delta\Phi$ changes with W_{si} for a 13-μm-long phase modulator. We also investigate the effect of the metal thickness on Δn_{re} and $\Delta\Phi$, as shown in Figs. 4(c) and 4(d). We choose polymer width $W_{\mathrm{polymer}} = 20\,\mathrm{nm}$ and Ag widths $W_{\mathrm{Ag}} = 10$, 20, and 50 nm. Δn_{re} does not change much as the Ag width decreases, so there is no need for accurate metal thickness control, which can simplify the fabrication process.

Considering the fabrication feasibility and modulation efficiency, the device geometric parameters can be chosen as $W_{\mathrm{Si}} = 100\,\mathrm{nm}$, $W_{\mathrm{polymer}} = 20\,\mathrm{nm}$, and $W_{\mathrm{Ag}} = 10\,\mathrm{nm}$. Figure 5 shows the that phase shift changes with the drive voltage for a 13-μm-long phase modulator. At 2.5 V drive voltage, the change in the real part of the effective refractive index is −0.06, which implies a $\sim\pi$ phase change from the modulator. The phase modulator insertion loss is ~10 dB, mainly coming from the hybrid plasmonic mode propagation loss.

C. Coupling to the Dielectric Waveguide

A silicon wire waveguide has a low propagation loss and is more suitable for optical transmission than the hybrid plasmonic waveguide. In order to connect the hybrid plasmonic waveguide to a silicon wire waveguide, we design adiabatic tapers at the input and output ends of the phase modulator. As shown in Fig. 1(a), the adiabatic tapers are also covered

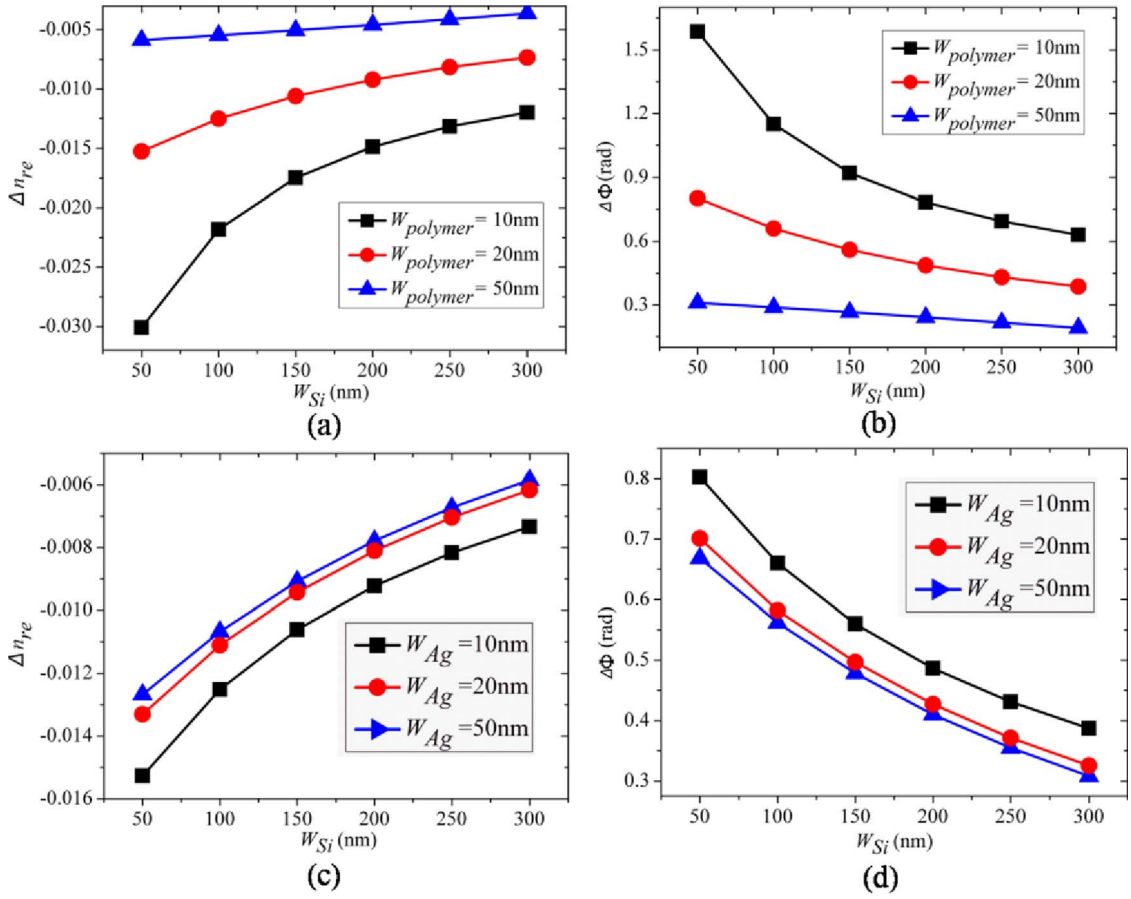

Fig. 4. (Color online) (a) and (b) Δn_{re} and $\Delta\Phi$ versus W_{Si} for $W_{\mathrm{polymer}} = 10$, 20, and 50 nm. $d = 13\,\mu$m and $W_{\mathrm{Ag}} = 10$ nm. (c) and (d) Δn_{re} and $\Delta\Phi$ versus W_{Si} for $W_{\mathrm{Ag}} = 10$, 20, and 50 nm. $d = 13\,\mu$m and $W_{\mathrm{polymer}} = 20$ nm.

with polymer and silver to enable a smooth mode transform. Optical energy is well confined in the silicon core for the silicon wire waveguide. When the silicon core tapers down, optical energy is gradually squeezed into the sidewall polymer layer. Because of the symmetry of the structure and the narrow silicon strip width (odd mode is under cutoff), eventually only the even mode is excited in the hybrid plasmonic waveguide. Adiabatic tapers require a long tapering length to minimize the mode transform loss. However, a long tapering length also means higher loss due to the silver absorption in the taper sections. Therefore, there exists an optimum taper length at which the coupling efficiency reaches the maximum. Figure 6(a) shows that the three-dimensional simulated transmission efficiency changes as a function of taper length. Here, the transmission efficiency η is defined as $\eta = P_{\mathrm{output}}/P_{\mathrm{input}}$, where P_{input} and P_{output} are the light input and output power. For a 1-μm-long plasmonic waveguide, the maximum transmission efficiency is ~68% for a taper length of 500 nm. Given that the hybrid plasmonic waveguide has a propagation loss of ~0.828 dB/μm [see Fig. 3(b)], the coupling efficiency of the taper is estimated to be ~91%. Figure 6(b) shows the top-view electric field propagation pattern in the device. A smooth mode transform from the silicon dielectric waveguide to the hybrid plasmonic waveguide is observed without obvious backreflection and diffraction in the taper sections.

D. Modulation Speed and Power Consumption

Given that the inherent response time of the polymer is of the order of femtoseconds [25], the capacitor charging and discharging time (RC time) is the limiting factor to the modulating speed of the device.

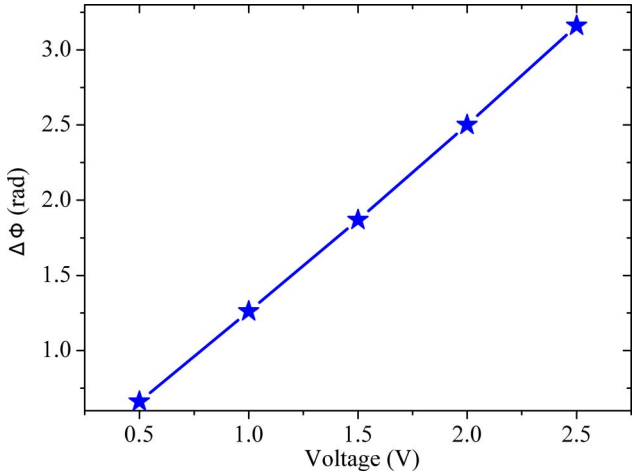

Fig. 5. (Color online) Phase shift of a 13-μm-long plasmonic waveguide versus drive voltage.

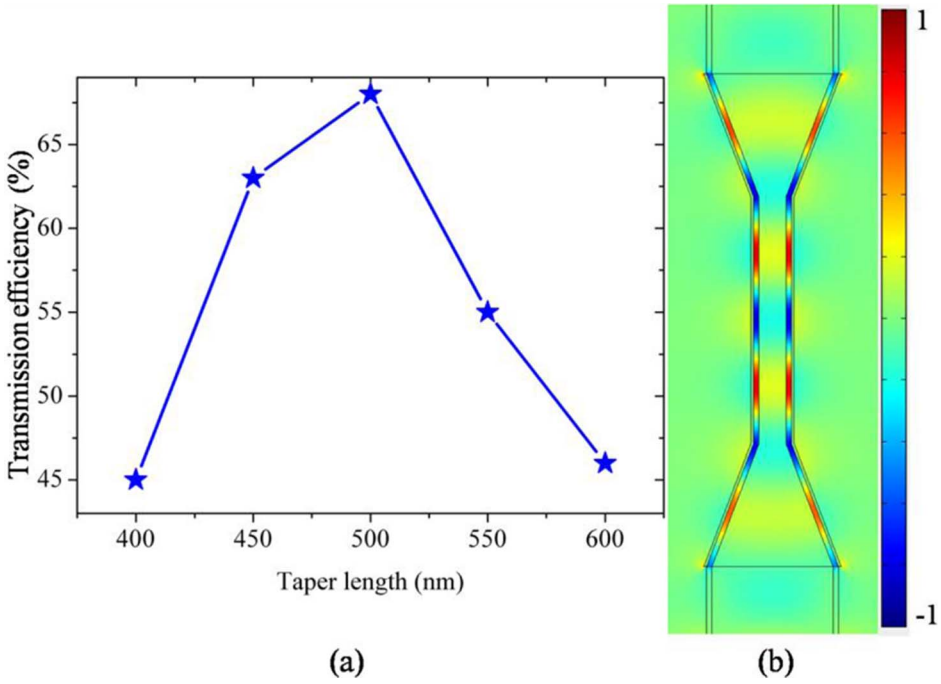

Fig. 6. (Color online) (a) Transmission efficiency versus taper length. (b) Electric field pattern showing the coupling from silicon waveguide to plasmonic waveguide. Waveguide parameters are chosen as $W_{Si} = 100\,nm$, $H_{Si} = 200\,nm$, $W_{Ag} = 10\,nm$, $W_{polymer} = 20\,nm$, and the SiO_2 cap layer thickness is 100 nm.

The silicon core, doped with phosphorus (concentration $2 \times 10^{20}\,cm^{-3}$), has a very low resistivity of $\rho = 4 \times 10^{-4}\,\Omega{\cdot}cm$. The doped hybrid plasmonic waveguide has a propagation loss of $\sim 0.828\,dB/\mu m$, of which $\sim 0.6\,dB/\mu m$ propagation loss comes from the metal absorption and the other from the free-carrier absorption. As shown in Fig. 1(a), in our device, the silicon core input and output ends are connected to one common electrode, which effectively reduces the resistance and increases the modulation speed. The parasitic resistance of the modulator is contributed by the plasmonic hybrid waveguide, the waveguide taper, the silicon access waveguide, and the finger-shaped connection bridges. The resistance can be calculated as $R = \rho l/s$, where ρ is the resistivity of the silicon layer, and l and s are the length and the cross-sectional area of the silicon strip, respectively. As the silicon core in the hybrid waveguide has a small cross section and a long length, it makes the largest contribution to the entire resistance (the others can be neglected). The resistance is thus estimated to be $1.3\,\Omega k$. The capacitance can be calculated by $C = \varepsilon s/d$, where ε is the permittivity of the polymer material, and d and s are the thickness and sidewall coverage area of the polymer layer. The capacitance is estimated to be 2.9 fF. Hence, the RC time is 3.77 ps, corresponding to a modulation bandwidth of ~100 GHz. The power consumption primarily comes from dynamically charging and discharging the capacitor. At 2.5 V applied voltage, the power consumption is $P = 0.5fCV^2 = 0.9\,mW$ (or equivalently 9 fJ/bit), assuming the modulation frequency is $f = 100\,GHz$. Compared to other modulator structures based on photonic crystal waveguides or slot waveguides [18,23], our proposed hybrid-plasmonic-waveguide-based phase modulators have the combined benefits of short device length, fast speed, large bandwidth, and low power consumption. The high performance of the modulator can satisfy the future requirements for fast modulation speed and low power consumption in optical telecommunication and interconnect applications.

4. Fabrication Feasibility

The proposed phase modulator can be realized by using existing fabrication technologies. Here we give a feasible fabrication process flow that can produce such a device. First, a thin SiO_2 layer is deposited by using plasma enhanced chemical vapor deposition on a standard silicon-on-insulator (SOI) wafer. The SiO_2 layer is then patterned by electron-beam lithography (EBL) followed by reactive ion etch. The patterned SiO_2 layer can then act as a hard mask for the underlying silicon layer dry etch. The silicon core doping can be done by ion implantation. Then a thin layer of polymer can be deposited on top by using molecular beam epitaxy to accurately control its thickness. The waveguide needs to be tilted in order to make the sidewall coverage possible. The deposited polymer is then patterned by EBL to cover only the plasmonic waveguide part. Finally, a thin layer of Ag is deposited on top by sputtering and patterned by lift-off to obtain the desired metal connection pattern. In order to enhance the electro-optic coefficient of the polymer, the polymer should be properly poled before device operation. The poling can be accomplished by applying a high electric field across

the polymer nanoslot layer using the patterned electrodes.

5. Conclusions

In summary, a plasmonic-waveguide-based optical phase modulator is proposed. The plasmonic waveguide is composed of silver–polymer–silicon stack layers to fully utilize the high confinement feature of the plasmonic mode and the high linear electro-optic effect of the polymer material. The optical field is strongly enhanced in the nanometer thin polymer layer for TE polarization. Upon a 2.5 V voltage, the plasmonic waveguide experiences a large effective refractive index change, causing an $\sim\pi$ phase shift for a 13-μm-long device. Because of its compact size, the modulation bandwidth can reach ~100 GHz and the power consumption is very low at 9 fJ/bit. The proposed phase modulator can find many applications in future power-hungry optical information processing modules for telecommunication and interconnects.

This work was supported in part by the 973 Program (2011CB301700), the National Natural Science Foundation of China (NSFC, 60877012, 61001074, 61007039), the Shanghai Leading Academic Discipline Project and the Science and Technology Committee of Shanghai Municipal (S30108 and 08DZ2231100), the Project of the Ministry of Education Key Lab of Optical Fiber Sensing and Communications (University of Electronics Science and Technology of China), and the Shanghai Jiao Tong University Innovation Fund For Postgraduates.

References

1. V. M. Agranovich and D. L. Mills, eds., *Surface Polaritons: Electromagnetic Waves at Surfaces and Interfaces* (Elsevier, 1982).
2. See the review of *Surface Polaritons: Electromagnetic Waves at Surfaces and Interfaces* by H. J. Simon, J. Opt. Soc. Am. B 1, 410 (1984).
3. D. Gramotnev and S. Bozhevolnyi, "Plasmonics beyond the diffraction limit," Nat. Photon. **4**, 83–91 (2010).
4. E. Moreno, F. J. Garcia-Vidal, S. G. Rodrigo, L. Martin-Moreno, and S. I. Bozhevolnyi, "Channel plasmon-polaritons: modal shape, dispersion, and losses," Opt. Lett. **31**, 3447–3449 (2006).
5. S. I. Bozhevolnyi, V. S. Volkov, E. Devaux, J. Y. Laluet, and T. W. Ebbesen, "Channel plasmon subwavelength waveguide components including interferometers and ring resonators," Nature **440**, 508–511 (2006).
6. D. F. P. Pile and D. K. Gramotnev, "Channel plasmon-polariton in a triangular groove on a metal surface," Opt. Lett. **29**, 1069–1071 (2004).
7. G. Veronis and S. Fan, "Guided subwavelength plasmonic mode supported by a slot in a thin metal film," Opt. Lett. **30**, 3359–3361 (2005).
8. L. Liu, Z. Han, and S. He, "Novel surface plasmon waveguide for high integration," Opt. Express **13**, 6645–6650 (2005).
9. D. F. P. Pile, D. K. Gramotnev, R. F. Oulton, and X. Zhang, "On long-range plasmonic modes in metallic gaps," Opt. Express **15**, 13669–13674 (2007).
10. E. Verhagen, A. Polman, and L. K. Kuipers, "Nanofocusing in laterally tapered plasmonic waveguides," Opt. Express **16**, 45–57 (2008).
11. R. F. Oulton, V. J. Sorger, D. A. Genov, D. F. P. Pile, and X. Zhang, "A hybrid plasmonic waveguide for subwavelength confinement and long-range propagation," Nat. Photon. **2**, 496–500 (2008).
12. M. Z. Alam, J. Meier, J. S. Aitchison, and M. Mojahedi, "Propagation characteristics of hybrid modes supported by metal-low-high index waveguides and bends," Opt. Express **18**, 12971–12979 (2010).
13. M. Fujii, J. Leuthold, and W. Freude, "Dispersion relation and loss of subwavelength confined mode of metal dielectric-gap optical waveguides," IEEE Photon. Technol. Lett. **21**, 362–364 (2009).
14. D. X. Dai and S. L. He, "Low-loss hybrid plasmonic waveguide with double low-index nano-slots," Opt. Express **17**, 16646–16653 (2009).
15. G. T. Reed, G. Mashanovich, F. Y. Gardes, and D. J. Thomson, "Silicon optical modulators," Nat. Photon. **4**, 518–526 (2010).
16. R. Soref and B. Bennett, "Electrooptical effects in silicon," IEEE J. Sel. Top. Quantum Electron. **23**, 123–129 (1987).
17. G. Cocorullo and I. Rendina, "Thermo-optical modulation at 1.5 μm in silicon etalon," Electron. Lett. **28**, 83–85 (1992).
18. J.-M. Brosi, C. Koos, L. C. Andreani, M. Waldow, J. Leuthold, and W. Freude, "High-speed low-voltage electro-optic modulator with a polymer-infiltrated silicon photonic crystal waveguide," Opt. Express **16**, 4177–4191 (2008).
19. P. Rabiei, W. Steier, C. Zhang, and L. Dalton, "Polymer microring filters and modulators," J. Lightwave Technol. **20**, 1968–1975 (2002).
20. P. Johnson and R. Christy, "Optical constants of the noble metals," Phys. Rev. B **6**, 4370–4379 (1972).
21. G. Wang, T. Baehr-Jones, M. Hochberg, and A. Scherer, "Design and fabrication of segmented, slotted waveguides for electro-optic modulation," Appl. Phys. Lett. **91**, 143109 (2007).
22. I. Avrutsky, R. Soref, and W. Buchwald, "Sub-wavelength plasmonic modes in a conductor-gap-dielectric system with a nanoscale gap," Opt. Express **18**, 348–363 (2010).
23. T. Baehr-Jones, B. Penkov, J. Huang, P. Sullivan, J. Davies, J. Takayesu, J. Luo, T.-D. Kim, L. Dalton, A. Jen, M. Hochberg, and A. Scherer, "Nonlinear polymer-clad silicon slot waveguide modulator with a half wave voltage of 0.25 v," Appl. Phys. Lett. **92**, 163303 (2008).
24. T. D. Kim, J. W. Kang, J. D. Luo, S. H. Jang, J. W. Ka, N. Tucker, J. B. Benedict, L. R. Dalton, T. Gray, R. M. Overney, D. H. Park, W. N. Herman, and A. K. Y. Jen, "Ultralarge and thermally stable electro-optic activities from supramolecular self-assembled molecular glasses," J. Am. Chem. Soc. **129**, 488–489 (2007).
25. L. R. Dalton, B. H. Robinson, A. K. Jen, P. Ried, B. Eichinger, S.-H. Jang, J. Luo, S. Liu, Y. Liao, K. A. Firestone, N. P. Bhatambrekar, D. Bale, M. A. Haller, S. Bhattacharjee, J. Schendel, P. A. Sullivan, S. Hammond, N. Buker, F. Cady, A. Chen, and W. H. Steier, "Organic electro-optic materials," Proc. SPIE **5621**, 93–104 (2004).